International Journal of Fluid Mechanics & Thermal Sciences
2024, Vol. 10, No. 3, pp. 45-56
https://doi.org/10.11648/j.ijfmts.20241003.11

Research Article

Homotopy Perturbation Method for Analyzing the Effect of Viscous Dissipation on Steady Natural Convection Couette Flow with Convective Boundary Conditions

Tafida Mohammed Kabir*, Tajuddeen Abdulganiyu

Department of Mathematics, Federal University of Education, Zaria, Nigeria

Abstract

This research article presents an analytical study of convective flow in a vertical channel with convective boundary conditions. Because of the nonlinear nature of the governing energy and momentum equations, the homotopy perturbation method was employed. The effects of various physical parameters on temperature and velocity profiles are illustrated in Figures 2 to 9, and a comparison table is provided to validate the results. Notably, both temperature and velocity distributions increased with higher viscous dissipation. Furthermore, the velocity profile decreased with an increase in the Biot number, while the temperature profile adjacent to the plate increased as the Biot number grew. Shear stress also exhibited an upward trend with rising viscous dissipation. Finally, an increase in the Grashof number and Biot number is found to elevate the skin friction on both plates. The mean temperature is higher when air is used as the working fluid compared to mercury. To validate this study, the temperature and velocity results were compared with previously published work, showing excellent agreement. This confirms the efficiency of the Homotopy Perturbation Method in solving coupled and nonlinear system of differential equations. Additionally, it was observed that both temperature and velocity increase with a rise in the Prandtl number, attributed to the dominance of momentum diffusivity over thermal diffusivity.

Keywords

Convective Boundary Condition, Couette Flow, Natural Convection, Viscous Dissipation, Homotopy Perturbation Method

1. Introduction

The study of natural convection in Couette flow has gained significant attention due to its applications in various fields, including engineering, geothermal energy, the petroleum industry, physics, nuclear power plants, and lubrication technology. Momohjimoh et al. [1] observed a reduction in velocity boundary layer thickness with increasing Biot and Prandtl numbers. Ajibade et al. [2] noted that greater internal conductive resistance diminishes buoyancy forces, resulting in reduced fluid thickness, temperature, and velocity. Agunbiade and Oyekunle [3] reported that higher viscous dissipation enhances fluid temperature and velocity. Similarly, Tafida and Ajibade [4] highlighted the positive influence of viscous dissipation on these parameters. Ajibade and Tafida [5] found that velocity boundary layer thickness enhances with larger Biot numbers.

Astanina et al. [6] demonstrated that variable viscosity in

*Corresponding author: mktafida.555@gmail.com (Tafida Mohammed Kabir)

Received: 7 November 2024; **Accepted:** 28 November 2024; **Published:** 23 December 2024

the working fluid effectively controls heat transfer and fluid flow. Hussain et al. [7] confirmed that the rate of heat transfer improves with higher Prandtl numbers. Ajibade et al. [8] revealed that hydrodynamic and thermodynamic distributions improve with increased viscous dissipation, while Ajibade and Tafida [9] observed that viscous dissipation raises fluid temperature but tends to reduce velocity. Finally, Ajibade and Princely [10] concluded that greater viscous dissipation leads to higher fluid temperature and velocity within the channel. Mehdi and Kourosh [11] concluded that growing the generalized Prandtl number increases heat transfer while reducing skin friction, and also decreases the thickness of the temperature boundary layer. Muawiya and Tafida [12] observed that the mass flux increases with higher viscous dissipation (Ec). Isa et al. [13] reported that skin friction rises with an increase in the Grashof number, while the Nusselt number decreases. Hamza [14] noted that the heat source parameter increases with a rise in the Biot number. Masthanaiah et al. [15] indicated that higher values of viscous dissipation result in greater temperature generation. Tafida et al. [16] concluded that velocity and temperature distribution develop as viscous dissipation increases.

Ajibade et al. [17] observed that the velocity profile decreases adjacent to the cold plate as viscous dissipation increases. Liu et al. [18] highlighted the superiority of their method over conventional approaches, emphasizing its flexibility in selecting the initial approximation. Abker [19] successfully provided solutions for both linear and nonlinear equations by the method of homotopy perturbation (HPM). Abu-Zeid [20] found that temperature rises with an increase in the Brinkman number. Adamu [21] concluded that HPM is a robust and effective tool for solving coupled differential equations. Ajibade and Tafida [22] demonstrated the effectiveness of their HPM-based solution, achieving excellent results. Nasution [23] reported that HPM is suitable for solving nonlinear differential equation systems, as evidenced by simulations where HPM results closely matched numerical simulations using the 4th-order Runge-Kutta method. The main objective of this research is to apply the homotopy perturbation method (HPM) to examine the impact of viscous dissipation on steady natural convection Couette flow under convective boundary conditions. The governing equations for this flow are coupled and nonlinear, making them suitable for numerical schemes or approximate solution methods. Among these, the perturbation method is effective; however, its solutions are limited to small perturbation parameters. To address this limitation, the homotopy perturbation method (HPM) is introduced as an alternative. HPM offers rapid convergence, often requiring only a limited terms in the series solution to achieve high correctness. Given the nonlinearity and coupling of the governing equations, HPM is employed in this study to solve the energy and momentum equations.

2. Methodology

We examine a steady flow of an incompressible fluid with viscous dissipation occurring between two vertical parallel plates positioned at specific locations. $y^* = 0$ and $y^* = h$, where the hot and cold walls are maintained at uniform temperatures T_1 and T_0, respectively. It is assumed that the flow occur in the x^* – direction, vertically upward along the plates, while the y^* – axis is perpendicular to the plates, as depicted in Figure 1. Given the infinite length of the plates, both the velocity and temperature fields are assumed to depend solely on the spatial coordinate. y^*.

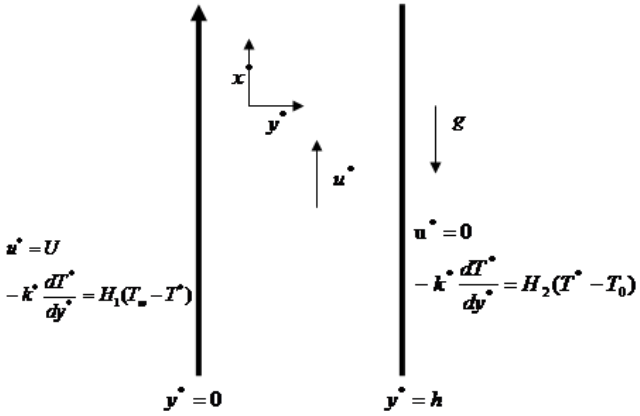

Figure 1. *Schematic diagram of the problem.*

The flow behavior and heat transfer in a vertical channel based on the Boussinesq's approximation, are described by the following governing equations:

$$\alpha \frac{d^2T^*}{dy^{*2}} + \frac{\mu^*}{\rho cp}\left(\frac{du^*}{dy^*}\right)^2 = 0, \tag{1}$$

$$\nu \frac{d^2u^*}{dy^{*2}} + g\beta\left(T^* - T_0\right) = 0. \tag{2}$$

The corresponding boundary conditions for these equations are:

$$u^* = U, \quad -k^* \frac{dT^*}{dy^*} = H_1(T_w - T^*) \quad \text{at} \quad y^* = 0$$

$$u^* = 0, \quad -k^* \frac{dT^*}{dy^*} = H_2(T^* - T_0) \quad \text{at} \quad y^* = h. \tag{3}$$

As the quantities involved have different dimensions, we introduce appropriate dimensionless variables to transform

the governing equations and boundary conditions into a dimensionless form. The dimensionless quantities used in equations (1) – (2) and boundary condition (3) are:

$$y=\frac{y^*}{h},\ u=\frac{u^*}{U},\ T=\frac{T^*-T_0}{T_w-T_0},\ Gr=\frac{g\beta h^2\left(T_w-T_0\right)}{\nu^2},$$

$$Ec=\frac{U^2}{c_p\left(T_w-T_0\right)},\quad \Pr=\frac{\mu cp}{k},\quad Bi=\frac{hd}{k} \tag{4}$$

Using these definitions, equations (1) to (3) can be rewritten in the following non-dimensional forms:

$$\frac{d^2T}{dy^2}+Ec\,\Pr\left(\frac{du}{dy}\right)^2=0, \tag{5}$$

$$\frac{d^2u}{dy^2}+GrT=0, \tag{6}$$

The non-dimensional boundary conditions are:

$$u=1,\quad \frac{dT}{dy}=Bi(T-1),\ \text{ at }\ y=0$$

$$u=0,\quad \frac{dT}{dy}=-BiT,\ \text{ at} \tag{7}$$

Method of Solution

To address the problem with the Homotopy Perturbation Method, we formulate a convex homotopy for the energy and momentum equations. As a result, the equations can be expressed in the following form without requiring an initial approximation:

$$\frac{d^2T}{dy^2}=p\left[-Ec\,\Pr\left(\frac{du}{dy}\right)^2\right] \tag{8}$$

such that

$$T=T_0+pT_1+p^2T_2+p^3T_3+... \tag{9}$$

By putting equation (9) into equation (8), we have

$$\frac{d^2T_0}{dy^2}+p\frac{d^2T_1}{dy^2}+p^2\frac{d^2T_2}{dy^2}+...=-p\left(Ec\,\Pr\left(\frac{du_0}{dy}\right)^2\right)-p^2\left(2Ec\,\Pr\left(\frac{du_0}{dy}.\frac{du_1}{dy}\right)\right)-p^3\left(2Ec\,\Pr\left(\frac{du_0}{dy}.\frac{du_2}{dy}-Ec\,\Pr\left(\frac{du}{dy}\right)^2\right)\right)-... \tag{10}$$

By relating the coefficient of $p^0, p^1, p^2, p^3...$, we obtain

$$p^0:\frac{d^2T_0}{dy^2}=0, \tag{11}$$

$$p^1:\frac{d^2T_1}{dy^2}=-Ec\,\Pr\left(\frac{du_0}{dy}\right)^2, \tag{12}$$

$$p^2:\frac{d^2T_2}{dy^2}=-2Ec\,\Pr\frac{du_0}{dy}.\frac{du_1}{dy}, \tag{13}$$

$$p^3:\frac{d^2T_3}{dy^2}=-2Ec\,\Pr\frac{du_0}{dy}.\frac{du_2}{dy}-Ec\,\Pr\left(\frac{du_1}{dy}\right)^2, \tag{14}$$

The boundary conditions are transformed to:

$$T_0'(0)=Bi(T_0-1),\quad T_1'(0)=BiT_1, T_2'(0)=BiT_2, T_3'(0)=BiT_3,...$$

$$T_0'(1)=-BiT_0, T_1'(1)=-BiT_1, T_2'(1)=-BiT_2, T_3'(1)=-BiT_3,... \tag{15}$$

Similarly, for equation (6), there is no initial approximation; thus, it can be transformed into:

$$\frac{d^2u}{dy^2} = p\left[\frac{dP}{dx} - GrT\right] \tag{16}$$

such that

$$u = u_0 + pu_1 + p^2u_2 + p^3u_3 + ... \tag{17}$$

By substituting equation (17) into equation (16), we obtain:

$$\frac{d^2u_0}{dy^2} + p\frac{d^2u_1}{dy^2} + p^2\frac{d^2u_2}{dy^2} + ... = -pGrT_0 - p^2GrT_1 - p^3GrT_3 - ... \tag{18}$$

By relating the coefficient of $p^0, p^1, p^2, p^3...$, we obtain

$$p^0 : \frac{d^2u_0}{dy^2} = 0\,, \tag{19}$$

$$p^1 : \frac{d^2u_1}{dy^2} = -GrT_0, \tag{20}$$

$$p^2 : \frac{d^2u_2}{dy^2} = -GrT_1, \tag{21}$$

$$p^3 : \frac{d^2u_3}{dy^2} = -GrT_2, \tag{22}$$

The boundary conditions for these equations are transformed to:

$$u_0(0) = 1,\quad u_1(0) = u_2(0) = u_3(0) = ... = 0,\ u_0(1) = 0, u_1(1) = 0, u_2(1) = 0, u_3(1) = 0..., \tag{23}$$

Thus, by solving equations (11) and (19) and applying the boundary conditions $T_0'(0) = Bi(T_0 - 1)$ and $T_0'(1) = -BiT_0$, $u_0(0) = 0,$ and $u_0(1) = 0,$ we obtain the solutions

$$T_0 = A_1y + A_2 \tag{24}$$

$$u_0 = B_1y + B_2, \tag{25}$$

Thus, by solving equations (12) and (20) and applying the boundary conditions $T_1'(0) = BiT_1$, and $T_1'(1) = -BiT_1$, $u_1(0) = 0,$ and $u_1(1) = 0,$ we obtain the solutions

$$T_1 = \frac{-Ec\,\mathrm{Pr}\,y^2}{2} + A_3y + A_4, \tag{26}$$

$$u_1 = \frac{GrBiy^3}{6(2+Bi)} - \frac{Gr(1+Bi)y^2}{2(2+Bi)} + B_3y + B_4. \tag{27}$$

Thus, by solving equations (13) and (21) and applying the boundary conditions $T_2'(0) = BiT_2$, and $T_2'(1) = -BiT_2$, $u_2(0) = 0,$

and $u_2(1)=0,$ we obtain the solutions

$$T_2=\frac{Ec\,\mathrm{Pr}\,GrBiy^4}{12(2+Bi)}-\frac{Ec\,\mathrm{Pr}\,Gr(1+Bi)y^3}{3(2+Bi)}+\frac{Ec\,\mathrm{Pr}\,Gr(1+Bi)y^2}{2(2+Bi)}-\frac{Ec\,\mathrm{Pr}\,GrBiy^2}{6(2+Bi)}+A_5y+A_6. \tag{28}$$

$$u_2=\frac{Ec\,\mathrm{Pr}\,Gry^4}{24}-\frac{A_3Gry^3}{6}-\frac{A_4Gry^2}{2}+B_5y+B_6. \tag{29}$$

Thus, by solving equations (14) and (22) and applying the boundary conditions $T_3^{'}(0)=BiT_3$, and $T_3^{'}(1)=-BiT_3$, $u_3(0)=0,$ and $u_3(1)=0,$ we obtain the solutions

$$T_3=\frac{Ec^2\,\mathrm{Pr}^2\,Gry^5}{60}-\frac{Ec\,\mathrm{Pr}\,GrA_3y^4}{12}-\frac{Ec\,\mathrm{Pr}\,GrA_4y^3}{6}+\frac{Ec\,\mathrm{Pr}\,A_3y^2}{6}+\frac{Ec\,\mathrm{Pr}\,Gry^2}{2}-\frac{Ec^2\,\mathrm{Pr}^2\,Gry^2}{24}-\frac{Ec\,\mathrm{Pr}\,Gr^2Bi^2y^6}{120(2+Bi)^2}$$

$$+\frac{Ec\,\mathrm{Pr}\,Gr^2Bi(1+Bi)y^5}{40(2+Bi)^2}+\frac{Ec\,\mathrm{Pr}\,Gr^2Bi^2y^4}{144(2+Bi)^2}+\frac{Ec\,\mathrm{Pr}\,Gr^2Bi(1+Bi)y^4}{24(2+Bi)^2}-\frac{Ec\,\mathrm{Pr}\,Gr^2(1+Bi)^2y^3}{12(2+Bi)^2}+\frac{Ec\,\mathrm{Pr}\,Gr^2(1+Bi)^2y^3}{12(2+Bi)^2}$$

$$-\frac{Ec\,\mathrm{Pr}\,Gr^2Bi(1+Bi)y^3}{36(2+Bi)^2}-\frac{Ec\,\mathrm{Pr}\,Gr^2Bi(1+Bi)y^3}{24(2+Bi)^2}+\frac{Ec\,\mathrm{Pr}\,Gr^2(1+Bi)^2y^3}{12(2+Bi)^2}-\frac{Ec\,\mathrm{Pr}\,Gr^2(1+Bi)y^2}{8(2+Bi)^2}+\frac{Ec\,\mathrm{Pr}\,Bi^2(1+Bi)y^2}{24(2+Bi)^2}$$

$$+\frac{Ec\,\mathrm{Pr}\,Gr^2Bi^2y^4}{144(2+Bi)^2}-\frac{Ec\,\mathrm{Pr}\,Gr^2Bi(1+Bi)y^3}{36(2+Bi)^2}+\frac{Ec\,\mathrm{Pr}\,Gr^2Bi(1+Bi)y^2}{24(2+Bi)^2}-\frac{Ec\,\mathrm{Pr}\,Gr^2Bi^2y^2}{72(2+Bi)^2}-\frac{Ec\,\mathrm{Pr}\,Gr^2Bi(1+Bi)y^4}{48(2+Bi)^2}+A_7y+A_8. \tag{30}$$

$$u_3=\frac{-Ec\,\mathrm{Pr}\,Gr^2y^6}{360(2+Bi)}+\frac{Ec\,\mathrm{Pr}\,Gr^2(1+Bi)y^5}{120(2+Bi)}-\frac{Ec\,\mathrm{Pr}\,Gr^2(1+Bi)y^4}{24(2+Bi)}+\frac{Ec\,\mathrm{Pr}\,Gr^2Biy^4}{72(2+Bi)}-\frac{A_5Gry^3}{6}-\frac{A_6Gry^2}{2}+B_7y+B_8. \tag{31}$$

Where,

$$A_1=\frac{-Bi}{(2+Bi)},A_2=\frac{(1+Bi)}{(2+Bi)},B_1=-1,B_2=1,$$

$$A_3=A_4Bi,A_4=\frac{1}{(2Bi+Bi^2)}\left[\frac{Ec\,\mathrm{Pr}\,Bi}{2}+Ec\,\mathrm{Pr}\right],$$

$$B_3=\frac{Gr(1+Bi)}{2(2+Bi)}-\frac{GrBi}{6(2+Bi)},$$

$$A_5=A_6Bi,$$

$$B_5=\frac{A_3Gr}{6}+\frac{A_4Gr}{2}-\frac{Ec\,\mathrm{Pr}\,Gr}{24},$$

$$A_6=\frac{1}{(2Bi+Bi^2)}\left[\frac{Ec\,\mathrm{Pr}\,GrBi^2}{12(2+Bi)}-\frac{Ec\,\mathrm{Pr}\,GrBi(1+Bi)}{6(2+Bi)}\right]$$

$$A_7=A_8Bi,$$

$$B_7 = \frac{Ec\,\mathrm{Pr}\,Gr^2}{360(2+Bi)} + \frac{Ec\,\mathrm{Pr}\,Gr^2(1+Bi)}{30(2+Bi)} - \frac{Ec\,\mathrm{Pr}\,Gr^2 Bi}{72(2+Bi)} + \frac{A_5 Gr}{6}$$

$$A_8 = \frac{1}{(2Bi+Bi^2)}\left[\frac{Ec^2\,\mathrm{Pr}^2\,GrBi}{40} - \frac{Ec\,\mathrm{Pr}\,GrA_3 Bi}{12} - \frac{Ec\,\mathrm{Pr}\,GrA_4 Bi}{3} + \frac{Ec\,\mathrm{Pr}\,Gr^2 Bi^3(1+Bi)}{120(2+Bi)^2}\right]$$

$$\left[-\frac{Ec\,\mathrm{Pr}\,Gr^2 Bi(1+Bi)^2}{24(2+Bi)^2} - \frac{Ec\,\mathrm{Pr}\,GrBi^3(1+Bi)}{24((2+Bi)^2} + \frac{Ec\,\mathrm{Pr}\,GrA_3}{3} + \frac{Ec\,\mathrm{Pr}\,GrA_4}{3}\right]$$

$$\left[+\frac{7Ec\,\mathrm{Pr}\,Gr^2 Bi^2(1+Bi)}{720(2+Bi)^2} - \frac{Ec\,\mathrm{Pr}\,Gr}{3} + \frac{Ec\,\mathrm{Pr}\,Gr^2(1+Bi)^2}{45} - \frac{Ec\,\mathrm{Pr}\,Gr^2(1+Bi)^2}{4}\right]$$

$$B_4 = B_6 = B_8 = 0,$$

The rate of heat transfer and skin friction Nu_0, Nu_1, τ_0 and τ_1 are expressed as follows:

$$\left.\frac{dT}{dy}\right|_{y=0} = \frac{-Bi}{(2+Bi)} + A_3 + A_5 + A_7,$$

$$\left.\frac{dT}{dy}\right|_{y=1} = \frac{-Bi}{(2+Bi)} - Ec\,\mathrm{Pr} + A_3 + A_5 + A_7 + \frac{Ec\,\mathrm{Pr}\,GrA_4}{2}$$

$$-\frac{Ec\,\mathrm{Pr}\,Gr^2 Bi^2}{45(2+Bi)^2} + \frac{Ec\,\mathrm{Pr}\,GrBi^2(1+Bi)}{12(2+Bi)^2},$$

$$\left.\frac{du}{dy}\right|_{y=0} = -1 + \frac{Gr(1+Bi)}{2(2+Bi)} - \frac{GrBi}{6(2+Bi)} + \frac{A_3 Gr}{6} + \frac{A_4 Gr}{2} - \frac{Ec\,\mathrm{Pr}\,Gr}{24}$$

$$+\frac{Ec\,\mathrm{Pr}\,Gr^2}{360(2+Bi)} + \frac{Ec\,\mathrm{Pr}\,Gr^2(1+Bi)}{30(2+Bi)} - \frac{Ec\,\mathrm{Pr}\,Gr^2 Bi}{72(2+Bi)} + \frac{A_5 Gr}{6},$$

$$\left.\frac{du}{dy}\right|_{y=1} = -1 + \frac{GrBi}{3(2+Bi)} - \frac{Gr(1+Bi)}{2(2+Bi)} + \frac{Ec\,\mathrm{Pr}\,Gr}{8} - \frac{5GrA_4}{6} - \frac{Ec\,\mathrm{Pr}\,Gr}{72(2+Bi)}$$

$$-\frac{Ec\,\mathrm{Pr}\,Gr^2(1+Bi)}{120(2+Bi)} + \frac{Ec\,\mathrm{Pr}\,Gr^2 Bi}{24} - \frac{A_5 Gr}{60}$$

To find the mass flux, $Q = \int_0^1 u dy$, we have

$$Q = \frac{1}{2} - \frac{GrBi}{24} + \frac{Gr(1+Bi)}{12} - \frac{Ec\,\mathrm{Pr}\,Gr}{80} + \frac{GrA_3}{24} + \frac{GrA_4}{12} + \frac{Ec\,\mathrm{Pr}\,Gr^2}{1008} + \frac{7Ec\,\mathrm{Pr}\,Gr^2(1+Bi)}{720(2+Bi)} - \frac{Ec\,\mathrm{Pr}\,Gr^2 Bi}{240} + \frac{GrA_5}{36}.$$

To obtain the mean temperature,

$$Q_m = \frac{\int_0^1 uTdy}{\int_0^1 udy}, \quad Q_m = \frac{1}{2} - \frac{GrBi}{24(2+Bi)} + \frac{Gr(1+Bi)}{12(2+Bi)} - \frac{Ec\,\mathrm{Pr}\,Gr^2}{2520(2+Bi)} - \frac{GrA_5}{24(2+Bi)} - \frac{Bi}{2(2+Bi)} + \frac{(1+Bi)}{(2+Bi)}$$

$$- \frac{Ec\,\mathrm{Pr}}{6} + \frac{A_3}{2} + A_4 + \frac{Ec\,\mathrm{Pr}\,GrBi}{60(2+Bi)} - \frac{Ec\,\mathrm{Pr}\,Gr(1+Bi)}{12(2+Bi)} \tag{32}$$

3. Results and Discussion

This section presents a discussion of the results obtained. The analytical solutions for temperature and velocity are displayed in graphs and analyzed for various values of the monitoring parameters. Moreover, the calculated numerical values for the rate of heat transfer, skin friction, mass flux, and mean temperature are provided in tables for further evaluation.

The temperature and velocity profiles for different values of Eckert number (Ec) is displayed in Figures 2 and 3. Both distributions increase with higher Eckert numbers, as the fluid's kinetic energy surpasses the boundary layer enthalpy difference. This intensifies convection currents, reducing fluid density and resulting in higher temperature and velocity profiles within the channel. It is also noted that the effect of the Eckert number on the temperature distribution is more pronounced near the cold plate.

The effect of the thermal buoyancy ratio (Gr) is shown in Figures 4 and 5. It is observed that the temperature distribution increases near the heated plate as the Grashof number increases, while a decrease occurs near the cold plate with rising Grashof number. Additionally, the Grashof number has no noticeable effect on the temperature distribution at the center of the channel. In Figure 5, the velocity distribution increases across the channel with higher Gr values, which is attributed to the buoyancy forces overpowering the viscous forces. This causes fluid particles in more energetic regions to move toward less energetic areas.

Figures 6 and 7 illustrate the effects of the Prandtl number (Pr) on the fluid's temperature and velocity distributions. It is observed that both temperature and velocity increase as the Prandtl number rises. This is due to the dominance of momentum diffusivity over thermal diffusivity. Physically, as the momentum diffusivity rate surpasses the thermal diffusivity, the fluid's boundary layer thickness increases, which enhances the convection currents within the channel, leading to higher temperature and velocity distributions.

Figures 8 and 9 illustrate the effects of the Biot number (Bi) on the velocity and temperature distributions, respectively. Figure 8 shows that temperature distribution increases nearby the heated plate as the Biot number rises, while it decreases near the cold plate with an increasing Biot number. In Figure 9, the velocity profile is observed to decrease as the Biot number increases. This behavior is due to the dominance of internal conduction resistance over external convection resistance, which affects heat transfer to the fluid, consequently reducing its temperature and weakening fluid motion.

Table 1 presents the computed numerical values for the rate of heat transfer at both plates. It is evident from the table that, the rate of heat transfer decreases at both plates as viscous dissipation increases. Furthermore, an increase in both the Prandtl number and viscous dissipation results in a higher rate of heat transfer.

Table 2 shows the calculated numerical values of skin friction at both plates. It is observed that an increase in the Grashof number and Biot number inclines to raise the skin friction at both plates.

Table 3 presents the mass flux values. Mass flux increases as the Biot number and Grashof number rise, while it decreases with an increase in the Prandtl number.

Table 4 shows the mean temperature values. The mean temperature is higher when the working fluid is air compared to mercury. Additionally, the mean temperature increases with rising Grashof and Biot numbers.

Validation of results

To validate this study, we compared our results for temperature and velocity with those of Muawiya and Tafida [12], finding excellent agreement, as presented in Table 5. This confirms that the Homotopy Perturbation Method is an effective approach for solving coupled and nonlinear differential equations. Additionally, to further substantiate our findings, we extended the work of Muawiya and Tafida [12] by introducing a different boundary condition, specifically the convective boundary condition. The comparison is outlined in Table 5.

4. Conclusion

This article examines the effect of viscous dissipation on steady natural convection Couette flow with convective boundary conditions, employing the homotopy perturbation method. The energy and momentum equations were solved, and the results were presented graphically and analyzed for various values of the governing parameters. The study concludes that:

Both temperature and velocity profiles rise with increasing viscous dissipation,

The velocity profile decreases as the Biot number increases,

A rise in the Prandtl number and viscous dissipation leads to an enhanced rate of heat transfer,

The mean temperature is greater when air is used as the working fluid compared to mercury.

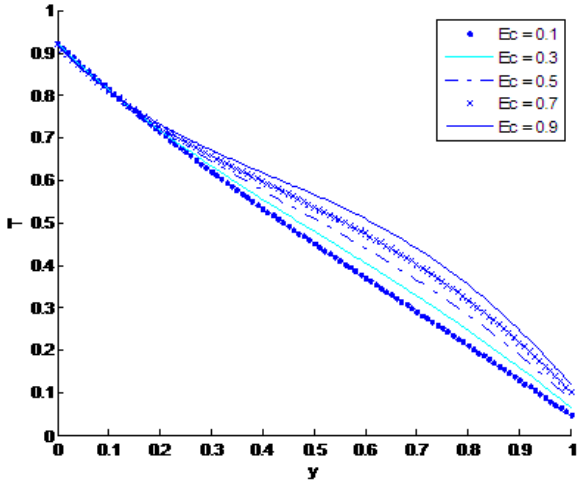

Figure 2. *Temperature profile for various values of* $Ec(\Pr = 0.71, Gr = 6.0, Bi = 15.0)$.

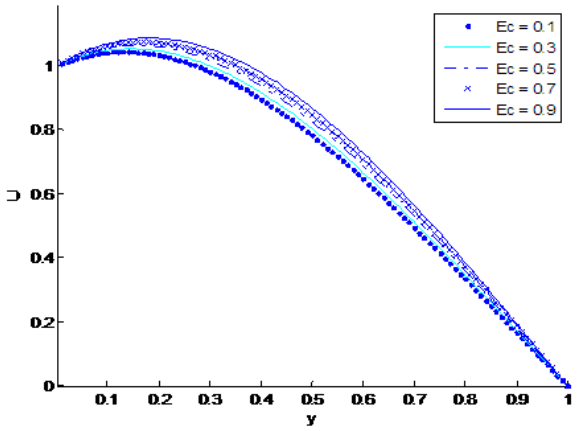

Figure 3. *Velocity profile for various values of* $Ec(\Pr = 0.71, Gr = 6.0, Bi = 15.0)$.

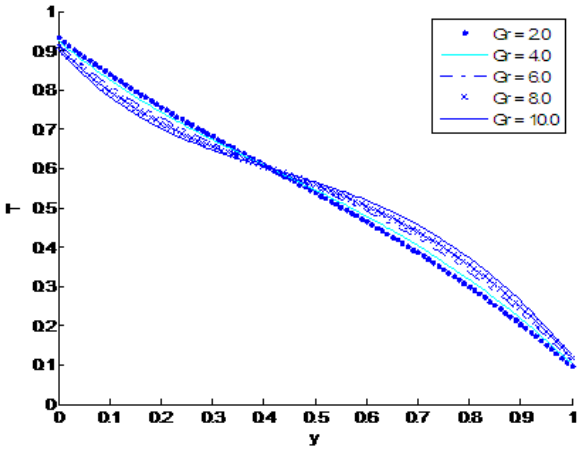

Figure 4. *Temperature profile for various values of* $Gr(Ec = 0.8, \Pr = 0.71, Bi = 15.0)$.

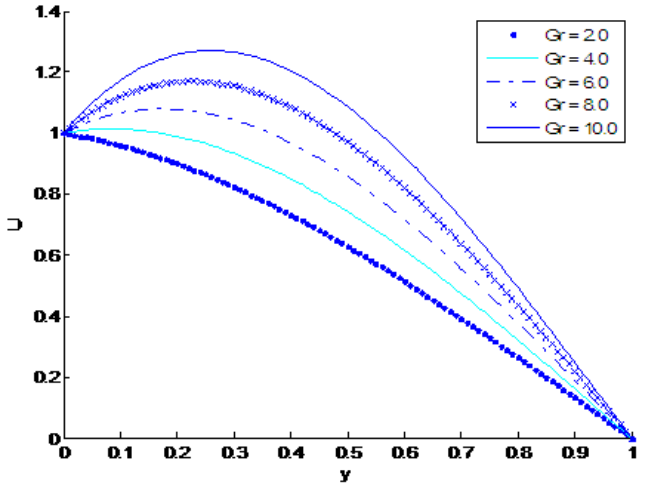

Figure 5. *Velocity profile for various values of* $Gr(Ec = 0.8, \Pr = 0.71, Bi = 15.0)$.

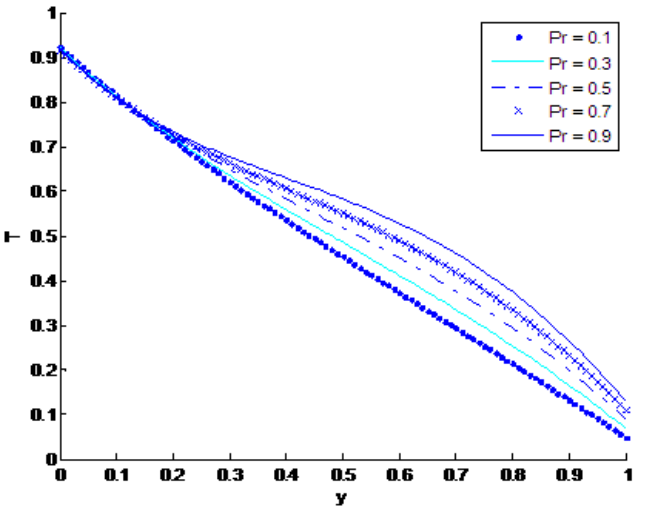

Figure 6. *Velocity profile for various values of* $\Pr(Ec = 0.8, Gr = 6.0, Bi = 15.0)$.

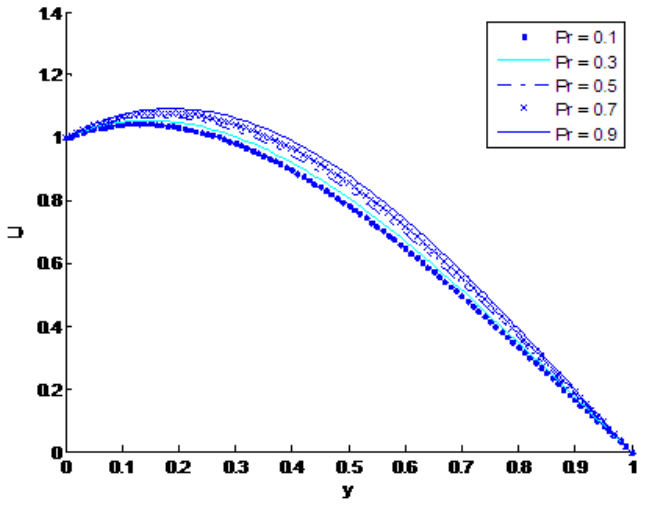

Figure 7. *Temperature profile for various values of* $\Pr(Ec = 0.8, Gr = 6.0, Bi = 15.0)$.

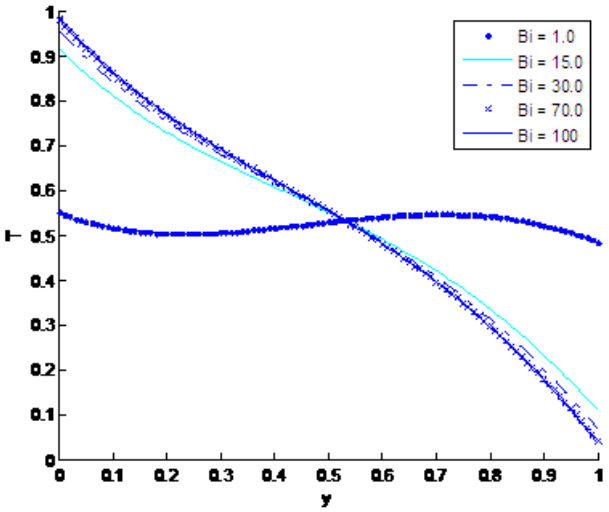

Figure 8. *Velocity profile for various values of* $Bi(Ec = 0.8, \Pr = 0.71, Gr = 6.0)$.

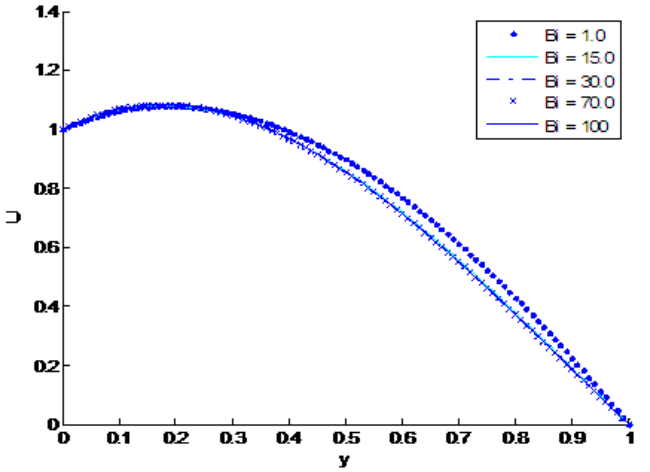

Figure 9. *Temperature profile for various values of* $Bi(Ec = 0.8, \Pr = 0.71, Gr = 6.0)$.

Table 1. *Calculated numerical values for the rate of heat transfer at both plates.*

		$Gr = 6.0, Bi = 7.0$		$Gr = 8.0, Bi = 7.0$		$Gr = 10.0, Bi = 17.0$	
Ec	**Pr**	Nu_1	Nu_0	Nu_0	Nu_1	Nu_0	Nu_1
0.1		0.6821	0.4346	0.6778	0.2668	0.4821	0.3353
0.4		0.3631	0.2538	0.3517	0.1287	0.3007	0.2078
0.7	0.044	0.2741	0.1780	0.2130	0.1007	0.2706	0.2006
1.0		0.0761	0.0431	0.0357	0.0927	0.1908	0.0990
0.1		0.5793	0.6110	0.4468	0.3700	0.4011	1.4462
0.4		0.2411	0.4240	0.1311	0.2356	0.2968	1.3207
0.7	0.71	0.1630	0.2086	0.1827	0.1971	0.2077	1.2006
1.0		0.0835	0.1781	0.1600	0.1736	0.1243	1.1371

Table 2. *Calculated numerical values for the skin friction at both plates.*

		$Gr = 6.0, Bi = 7.0$		$Gr = 8.0, Bi = 7.0$		$Gr = 10.0, Bi = 17.0$	
Ec	**Pr**	τ_1	τ_0	τ_0	τ_1	τ_0	τ_1
0.1		0.5261	1.6732	0.5273	1.6821	1.3281	1.5281
0.4		0.5700	1.7260	0.5738	1.7386	1.5711	1.6525
0.7	0.044	0.6134	1.9980	0.6380	1.9990	1.7013	1.9752
1.0		0.6531	2.3600	0.6597	2.4987	1.8245	2.3655
0.1		0.4217	1.4894	0.4256	1.4910	0.8525	1.0992

		$Gr = 6.0, Bi = 7.0$		$Gr = 8.0, Bi = 7.0$		$Gr = 10.0, Bi = 17.0$	
Ec	Pr	τ_1	τ_0	τ_0	τ_1	τ_0	τ_1
0.4		0.4530	1.5360	0.4620	1.5470	1.0710	1.3553
0.7	0.71	0.4986	1.8671	0.5211	1.8710	1.5051	1.8520
1.0		0.5246	1.9876	0.5632	1.9940	1.5652	2.2505

Table 3. *Calculated numerical values of mass flux* Q .

		$Gr = 6.0, Bi = 7.0$	$Gr = 8.0, Bi = 7.0$	$Gr = 8.0, Bi = 7.0$
Ec	Pr	Q	Q	Q
0.1		0.7685	0.7692	0.8235
0.4		0.7812	0.7850	0.8857
0.7	0.044	0.8150	0.8171	0.8891
1.0		0.8301	0.8380	0.9521
0.1		0.7445	0.7451	0.7425
0.4		0.7581	0.7598	0.7901
0.7	0.71	0.7805	0.7820	0.8873
1.0		0.8133	0.8182	0.849

Table 4. *Calculated numerical values of mean temperature* Q_m .

		$Gr = 6.0, Bi = 7.0$	$Gr = 8.0, Bi = 7.0$	$Gr = 8.0, Bi = 7.0$
Ec	Pr	Q_m	Q_m	Q_m
0.1		8.7552	8.7926	8.9572
0.4		4.0361	4.0675	4.2531
0.7	0.044	3.8501	3.9172	3.9721
1.0		5.8424	5.9715	6.2140
0.1		10.2706	11.6981	12.2531
0.4		5.2961	6.3284	7.9602
0.7	0.71	4.5072	5.7561	6.4821
1.0		6.8721	7.8815	8.1236

Table 5. Comparison of calculated numerical values between the present problem and that of Muawiya and Tafida [12].

	Muawiya and Tafida [12]		Present problem	
	$Gr = 6.0, \Pr = 0.71, y = 0.5$		$Gr = 6.0, \Pr = 0.71, Bi = 130, y = 0.5$	
Ec	Temperature	Velocity	Temperature	Velocity
0.1	0.4824	0.7761	0.4817	0.7703
0.4	0.4607	0.7538	0.4601	0.7510
0.7	0.4210	0.7210	0.4178	0.7193
1.0	0.3986	0.6993	0.3952	0.6907

Abbreviations

g	Acceleration to Due Gravity [ms^{-2}]
β	Coefficient of Thermal Expansion [K^{-1}}
h	Width of the Channel [m]
μ	Coefficient of Viscosity [$Kgm^{-1}s^{-1}$]
T^*	Dimensional Fluid Temperature [K]
ν	Kinematic Viscosity [m^2s^{-1}]
T_w	Channel Wall Temperature [K]
Pr	Prandtl Number
T_0	Temperature of the Ambience [K]
Gr	Grashof Number
T	Dimensionless Fluid Temperature
Ec	Eckert Number
u^*	Dimensional Velocity [ms^{-1}]
Bi	Biot Number
u	Dimensionless Velocity
c_p	Specific Heat at Constant Pressure [$m^2s^{-2}K^{-1}$]
U	Dimensional Velocity of the Moving Plate [ms^{-1}]
ρ	Density of the Fluid [Kgm^{-3}]
y^*	Coordinate Perpendicular to the Plate [m]
α	Thermal Diffusivity of the Fluid [Kgm^{-3}]
y	Dimensionless Co-ordinate Perpendicular to the Plate

Conflicts of Interest

The authors declare no conflicts of interest.

References

[1] Momohjimoh, S. A., Oyem, O. A., Momoh, O. S., Onojovwo, T,. Felix. Convective heat and casson nanofluid flow over a vertical plate with heat source. Fudma Journal of Sciences. (2023), 7(2); 9 – 18.

[2] Ajibade, A. O., Jeremiah, J. G., and Basant, K. J. Effect of darcy and viscous dissipation on natural convection flow in a vertical tube partially filled with porous material under convective boundary condition. International Journal of Applied Computational Mathematics. (2024), 10 – 84.

[3] Agunbiade, S. A., and Oyekunle, S. A. Effects of magnetic field on natural convective steady flow past an irregular vertical channel in the presence of viscous dissipation. FUW Trends in Science and Technology Journal. (2019), 4(3); 666 – 670.

[4] Tafida, M. K. and Ajibade, A. O. Variable viscosity and viscous dissipation effects on free convective Couette flow in a vertical channel: the homotopy perturbation method approach. (2020). The Journal of the Mathematical Association of Nigerian. 47(1), 161 – 175.

[5] Ajibade, A. O., Tafida, M. K. Viscous dissipation effect on steady natural convection Couette flow with convective boundary condition. International Journal of Non-linear Sciences and Numerical Simulation. (2022), https://doi.org/10.1515/ijnsns-2021-0055

[6] Astanina, M. S., Mikhail, A. S. numerical study on natural convection of fluid with Temperature dependent viscosity. International Journal of Thermofluids. 2023, 100266.

[7] Hussain, A., Isah, B. Y., and Zayyanu, S. Y. Impression of some fluid flow possession on unsteady conductive free convective fluid on account to dissipative porous walls. Himalayan Journal of Applied Medical Sciences and Research. 4(7), (2022), 31-52.

[8] Ajibade, A. O., Ayuba, M. U., and Tafida, M. K. An analytical study on effects of viscous dissipation and suction/injection on a steady MHD natural convection Couette flow of heat generating/absorbing fluid. Advances in Mechanical Engineering. 13(5), (2021), 1-12.

[9] Ajibade, A. O. and Tafida, M. K. Viscous dissipation effect of on steady natural Convection Couette flow with convective boundary condition. International Journal of Non-Linear Sciences and Numerical Simulation (IJNSNS). (2022), 7: 105 – 116.

[10] Ajibade, A. O. and Princely, O. O. Effect of viscous dissipation on steady natural convection, heat and mass transfer in a vertical channel with variable viscosity and thermal conductivity. Journal of Heat and Mass Transfer Research. (2020). 7: 105 116.

[11] Mehdi, M. and Kourosh, J. Viscous dissipation effect in the free convection of Non- Newtonian fluid with heat generation or absorption effect on the vertical wavy surface. Hindawi Journal of Applied Mathematics ID: 7567981, 14 pages. (2021): https//doi.org/10.1155/2021/7567981

[12] Muawiya, H. U. and Tafida, M. K. Viscous dissipation effects on steady natural convection Couette flow in a vertical channel. Wudil Journal of Pure and Applied Sciences. (2019), 1(2), 169 – 179.

[13] Isa, B. U., Yale, I. D., Sarki, M. N., and Hamza, M. M. Effects of viscous dissipative fluid on Couette flow in a vertical channel due to Newtonian heating. International Journal of Science for Global Sustainability. (2024), https//doi.org/10.57233/ijsgs.v10i1.595

[14] Hamza, M. M. Navier slip and convective boundary condition effects on transient combined convection of dissipative fluid. The Transactions of the Nigerian Association Mathematical Physics. (2023), vol 19 (Jan – Dec issues).

[15] Masthanaiah, Y., Nainaru, T., Ijaz, K. M., Rushikesava, S. M., Bandar, M. F., Sherzod, S., Abdullaer, S., and Sayed, M. E. Impact of viscous dissipation and entropy generation on cold liquid via channel with porous medium by analytical analysis. Case Studies in Thermal Engineering. (2023), 47; 103059.

[16] Tafida, M. K., Ayuba, M. U., and Lawal, U. Magnetohydrodynamics free convection Couette flow and heat transfer through a vertical porous plate with heat generation and absorption effects. Dutse Journal of Pure and Applied Sciences. (2023), 9(2a); 133 - 145.

[17] Ajibade, A. O., Ayuba, M. U. and Tafida, M. K. An Analytical study on effects of viscous dissipation and suction/injection on a steady MHD convection Couette flow of heat generating/absorbing fluid. Advances in Mechanical Engineering. (2021). 13(5), 1 – 12.

[18] Liu, Z. J., Adamu, M. Y., Suleiman, E., and He, J. H. Hybridization of Homotopy Perturbation method and Laplace transformation for the partial differential equations. Thermal Science. (2017), 21; 1843 – 1846.

[19] Abker, A. H. Solution of the linear and nonlinear Schrodinger equations using Homotopy Perturbation method and Iterative method. American Journal of Engineering Research. (2017), 6(3); 107 – 114.

[20] Abou-Zeid, M. Homotopy Perturbation Method for Magnetohydrodynamics Non-Newtonian Nanofluid flow through a porous medium in eccentric annuli with peristalsis. Thermal Science. (2017), 21(5); 2069 – 2080.

[21] Adamu, A. Y. Parameterized Homotopy Perturbation method. Nonlinear Science Letter A. (2017), 8(2); 240 – 243.

[22] Ajibade, A. O. and Tafida, M. K. Effects of variability in viscosity and thermal conductivity Couette flow and heat transfer. Transactions of NAMP vol. 11, (January – June, 2020 Issue).

[23] Nasution, H. Exploring of homotopy perturbation method (HPM) for Solving Spread of Covid-19. Jambura Journal of Biomathematics. (2023), 4(2); 138 – 154.